

Precise and Robust Iris Segmentation in Specular Noisy Iris Images for Iris Biometrics

Pandu J¹, Murali Krishna N², B. Prabhakar³

^{1,2}Dept. of ECE, Sreyas Institute of Engineering and Technology, Nagole, Hyderabad, India

³Dept. of ECE, JNTUH College of Engineering, Jagtial, Telangana, India

Corresponding E-mail: Pandu427@gmail.com¹

Email: muraliomkrish@gmail.com², bprabhakar2008@gmail.com³

Abstract

Precise and Accurate segmentation of iris itself is the major challenge encountered in the process of successful implementation of iris recognition system. Number of researchers invented numerous methods to segregate the iris portion from the captured image but noises like occlusions, eyelids and specular reflections are throwing challenges in the extraction of iris part from the eye image. Most of the algorithms used in segmentation of iris are based on edge information. Here in this proposal, we are bidding an automated iterative active contour model on the database provided by CASIA-Iris-1000, for the segmentation of the iris portion. Proposed segmentation algorithm resulted 99.6% accuracy in segregating the iris on the challenging CASIA_Iris_1000.

Keywords: Pupil detection, Limbiac detection, Specular reflection removal, Iterative intensity threshold with circularity estimation, Distance adaptive illumination compensation inpainting technique.

1. Introduction

Spread of digital technology in every sector of life made human survival a cinchy task for many transactions in communications, travelling, navigation, transport, technology, business, and commerce. But negative shade of technology accentuates the need of security in its utilization as the technological growth paved way to the unethical hacking and duplication of originals. In this scenario fake ID is the most exigent problems threatening society, creating troubles in the activities like cyber crime, terror attacks, and forgery in property documents. To avoid these malfunctions and fake IDs, automated personal identification systems using biometrics came into existence overcoming the drawbacks of traditional identification systems based on cards or passwords like. Structures like freckles, filaments, stripes, pupil controlling muscles, crypts, pigment frills, radial furrows, collarette etc. gives greater randomness and rich visible features to the iris pattern. Because of these randomly distributed microstructures, the iris pattern becomes unique and makes the pattern. Variability to a very high degree among different individuals. Ease of mathematical modeling, stability in pattern and high reliability makes iris recognition one of the popular biometrics for personal authentication and identification. An automatic segmentation algorithm to isolate the iris portion from the eye images taken from the CASIA database[2,31] is presented in this paper and compares accuracy with other prominent algorithms. The human eye is an organ with a complex system for the development of human vision and a spherical form with a radius of around 1.3 cm [1,30]. Basically, the eye structure can be broken down into three layers. 1. outer layer, consisting of multilayered cornea and limbus-connected sclera, choroid, ciliary body and iris are the 2. middle layer. The 3rd inner layer is the retina, which is light sensitive and transforms light. The apparent iris is an area of zigzag collarette between the ciliary and pupillary areas. The thickest area in the iris where the muscles of the sphincter and dilator overlap each other is Collarette. In the visible eye, the darkest portion is the pupil, an opening that controls the amount of light entering the retina. In brightly lit situations, when circular sphincter muscles are drawn towards the middle, the pupil is constricted and the amount of light entering the

retinal region is decreased. It becomes diatriac in dimly lit conditions as radial dilator muscles pull away from the middle, dilate the pupil and try to allow full light into the retina, as shown in figure 3.

The idea of using iris for identifying human was proposed by Flom and Safer in the paper published in the year 1957. when human eye is captured by the camera most of the time it is not possible to focus the iris part only. Normally eyelids, eyebrows and some part of nose and forehead will become the part of the acquired image. When iris is the only part that can be utilized for identification purpose, other areas like eyelids and eyebrows will become unwanted data and are required to be removed. Iris recognition system is mainly composed of four divisions, image acquisition, segregation of iris, extraction of features and matching. In these modules, the success rate of iris recognition highly depends on the accuracy of segregation of iris part for the acquired image. In this way segmentation of iris region is of prime interest. In literature Daugman's integro differential operator and wilde's circular haugh transform algorithms are highly popular in extracting the iris region from the acquired image. Mean while W. Boles, B. Boashash [4,7], W. K Kong and D. Zhang [3,8], Li Ma, et.al. [5,9] also gave some of the best algorithms in the domain of iris segmentation.

For Hough transform the data requirement is very high and at the same time it takes number of iterations to find the circular regions. Since for locating pupil boundary and iris boundary the same transform is used, the requirement of computations become hazardous and results in reduction of speed in real time applications. One more disadvantage is the requirement of threshold settings. Hough transform requires threshold values to be set for edge detection which sometimes may skip the edge points resulting in failure to detect circular edges. Many of the approaches involve pre-setting edge detection thresholds that minimize the robustness of changes in image strength. S suggested an automatic threshold for binarizing and assessing the pupil center on the histogram. P. Narote and A. From S. Narote, L. M. Waghmare [6,14] on the CASSIA V1 database, where the pupil area is processed and the database was processed to remove specular reflections. Here we propose some iris segmentation algorithms from the eye image, which are responsible for determining the pupillary boundary, limbiac boundary and removing unwanted data. The different phases required for iris segmentation are shown in the flow chart shown in Figure 1.

2. Proposed Segmentation Approach

When the experiment is put on large database, sophisticated procedures may yield erroneous results if proper care is not taken. To make the system robust, the procedures and assumptions that are considered should be highly acceptable and simple to implement. In case of eye images where the pictures are captchured for the men and women who were wearing contact lenses or spectacle glasses, the implementation of regular procedures may fail to give accurate results [10,11]. A non parametric fast approach algorithm is proposed for automatic segmentation of the iris from the given eye image by defining the pupil and limbus boundaries as circular or nearly circular i.e elliptical to some extent[12,13]. To extract the iris region which is lying between pupil and sclera, basically it is required to determine the pupillary and limbiac boundaries which are inner and outer borders of the iris [18,19].

Here a novel Iterative Intensity Threshold with Circularity Estimation (IITCE) procedure is proposed to mark pupillary boundary and Active Contour Weighted Post Mean Substitution (ACWPMS) method to approximate limbiac boundary [15,20]. Inside the whole eye image pupil region will be the darkest part and the gray level of this region will be very low and hence easy to extract the region space based on gray level intensity of existing pixels rather than using complicated procedures. But when images are captured from the camera, the intensity levels will not be uniformly spread across the image and at the same time gray level values of pixels of same eye will differ from image to image as they were captured under different illumination conditions. It creates problem in defining fixed threshold in the extraction of pupil region for the entire database images. In this regard enhancing the population of dark pixels in the pupil region and getting it detected with adaptive threshold is one of the solutions to segregate the pupil. To avoid the constraints on the intensities of the images, the image is darkened in steps to increase the pupil pixel population.

LED light used to illuminate eye, to capture the image also creates problem in detecting the pupil, as it will not spread light uniformly and the focus is mainly on iris region. The illumination will diminish as it moves away from the iris region to the corners. making the corners of the image much darker when compared to the centre region of the image. These dark pixels at corners are big obstacles as noise, in the separation of the pupil region from the image. Sometimes, gray levels of pixels defining the pupil region befall to be non uniform as their intensities vary in a random way because of specular reflections of light source. This creates a need to poise the pixel intensity levels of this region to be uniform, to make up the complete shape of the pupil. Here the proposed segmentation module is divided into three sub sections are preprocessing, Pupil detection and Limbiac detection.

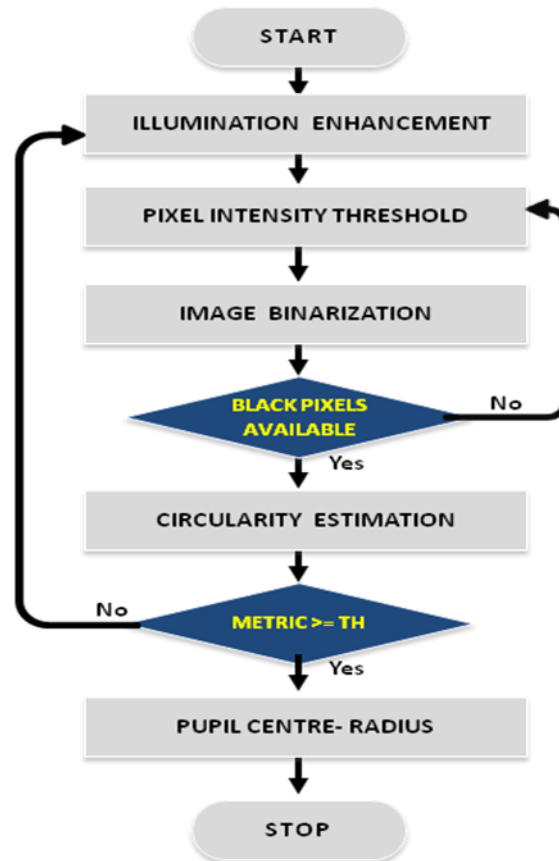


Figure 1. Pupil detection algorithm as a flow chart

2.1. Preprocessing

The fundamental assignment of preprocessing is to prepare the iris image into suitable form for segmentation of iris. Current days, for various reasons, lot of people are wearing spectacles which are compiling a great deal of specular reflection into the imaging and making segmentation task even more complicated. In this stage, denoising, detection and removal of specular reflections and intensity balancing of image pixels are some of the tasks to be carried.

2.1.1. Specular Reflection Removal

CASIA database contains specular reflections in and around the periphery of pupil region because of the LED light illumination, which baffles the segmentation of pupil region. Painting is one of the methods used to morph these reflections with the information available from the neighborhood pixels. The main intension of the proposed approach is not to reconstruct the image information at the positions of pixels, but to substantiate and nullify the effect of this kind of noise for precise segmentation of iris. Specular reflections, which are produced by LED illumination, are nothing but bright spots in the image, scaling gray values towards the white region. Many a time pixel intensity in the specular spot may not be uniform and create problems for the accurate detection of pupil region. Simple thresholding technique can be used to detect specular reflections within the image, considering

a pixel as a contributive sector of specular reflection if the intensity of the pixel is greater than some threshold limit (T). In the proposed approach, 80% of maximum value of the brightest pixel in the image is taken as threshold limit to identify the spots of specular reflections.

Since the candidate pixel values are non uniform, the pixels surrounding them may skip away from threshold conditions and remain creating trouble in detecting the pupil. So, it is evident to remove all these pixels by searching in the neighborhood of candidate pixel and nullify their effect. Sometimes the regions or spots in the image which are overexposed to light may also be considered as specular reflections erroneously. So much care is required in discrimination. Let I be the intensity of pixel I(x, y) at a location (x, y). let I_{max} be the maximum value of the brightest pixel in the image. In the proposed approach, a mask is generated for identifying specular reflections based on thresholding limit. The threshold limit (T) is computed as 80% of I_{max} value. If the intensity value of pixel (I) is greater than threshold value (T), the pixel is considered as a specular reflection.

Once specular reflections are identified, they were put for treatment individually based on their location in the image. Primarily, the intensities of candidate pixels and their neighborhood pixels are reduced to 30% of their individual values. In the second stage, the intensity values of the candidate pixel along with its eight neighborhoods are substituted with the average value of the group of pixels defined by a square block of size 11x11 with seed pixel at its centre. The procedure of specular removal with inpainting technique can be notified with the following steps.

- a. Notify the candidate pixels contributing for specular reflections by selecting the pixels whose intensities are less than the threshold value (T).
- b. Label the specular smudges.
- c. Remove large smudges with suitable threshold.
- d. Notify the pixel locations of candidate pixels in the input image and prepare the mask.
- e. Reduce the intensity of the candidate pixel by subtracting 70 % of its own value.
- f. Pick eight neighborhood pixels around the candidate pixel and repeat the procedure.
- g. Repeat the above procedure for all the candidate pixels of the generated mask.
- h. Replace the values of all individual pixels in the mask with mean of their neighborhood block of size 11x11.

2.1.2. Image Intensity Balance

For the databases like Casia Iris Thousand, Casia Iris Lamp, the illumination is not evenly distributed throughout the image where the corners of the image are darker to its central region. A radial operator is proposed to balance this difference of illumination, which scans the image in circular manner from the centre of the image and increases the intensity of pixels in reasonable steps. Two parameters that are required to start the operation are Coordinates of centre of the image and Intensity quotient by which illumination to be enhanced. Computation of centre coordinates of an image can be done simply by dividing the rows and columns of the image. i.e $x_{center} = rows / 2$; $y_{center} = columns / 2$. Intensity quotient by which each pixel on radial circle to be incremented is computed by dividing the difference of mean of outer region to centre region, with number of radial lines from centre to extreme boundary of image. The circular region with radius equal to half of the height of the image will be considered as inner region and the remaining area is considered as outer region.

$$I = \frac{(m_i - m_o)}{n} \quad (1)$$

Where, I Intensity quotient m_i and m_o are the average intensity values of inner and outer regions. 'n' is the number of radial lines.

Algorithm:

- a. Compute the centre of the image $c(x,y)$.

- b. Compute the intensity quotient I by using the difference of mean intensities of inner and outer regions.
- c. With $c(x,y)$ as centre and r as radius, scan the pixels along the circular paths and enhance the pixel intensities by an amount of illumination factor.
- d. Repeat the procedure with increment in radius r , taking values from 1 to n .

2.1.3. Denoising

Noise is one which may affect the segmentation process a lot as it may destroy the right informative pixels in the image. So, removal of noise from the eye image is must to attain good precision in iris segmentation. For denoising, a two-dimensional adaptive median filter which identifies the impulses by calculating the difference between the standard deviation of the pixels inside the filter window with the particular candidate pixel is applied.

2.2. Pupil detection

Iterative Intensity Threshold with Circularity Estimation (IITCE) is a two-layer iterative method used to achieve fast and effective segmentation of pupil by reducing the search area along with iterative intensity thresholding and circularity estimation of dark pixel cloud of pupil.

Algorithm:

- a. Input the preprocessed eye image I_{in} . Rescale the image to reduce mathematical complexity and time.
- b. Measure the intensity of image based on their mean value.
- c. Binarize the image based on pixel intensity threshold.
- d. Check for the cluster of dark pixels, contributing for pupil region.
- e. If they exist sufficiently, check for circularity otherwise increase the pixel intensity threshold, in steps, put for binarization of the image and continue to find it from step 3.

If the cluster of pupil pixels was found, and if the metric for circularity is within the threshold limit, accept it as pupil else change the illumination of image and continue from step 2. Once the pupil region was defined, find the centre and radius of pupil down scaling: First image is resized to one eighth of its original size, to obtain low resolution image over which pupil is approximated and can be refined back on to high resolution images later, thus significantly increasing segmentation speed and minimizing computational mathematics. Probing of region of interest: A circular contour is framed around the iris in such a way that iris area lies within the contour space. i.e., the iris region should be within the contour space so that the search area to detect pupil will be minimized.



Figure 2. Sequence of operations in pupil detection

2.2.1. Binarization

The input image is converted into binary image with a given threshold so that the pixels whose intensities lie below the threshold will be made 0 and all the remaining pixels to 255 of gray value. After binarization the image is complimented to form I_{com} . Finding connected components: Applying

some morphological operations, small noisy pixel blocks are removed to form image I_{open} . By using dilation and erosion operations on I_{open} , noise inside the components is removed and image I_{fill} is generated.

Estimation of compactness: Once the image I_{fill} is generated, the connected components in the image are labeled. Every component that is labeled will be tested for its compactness. Compactness Metric (CM) is defined to measure the circularity of the object with the equation

$$CM = \frac{4A\pi}{(P)^2} \quad (2)$$

Where, A is the area and P is the perimeter of the individual component. $CM=1$, defines unit metric. Unit metric defines full circularity to the object and measure towards zero defines deterioration in objects' circularity. Since not all the pupils are circular in nature, metric threshold is decreased gradually in steps for defined object in measuring its circularity and for the reasonable threshold condition the candidate pupil region is determined automatically.

2.2.2. Detection of pupil centre

Once the pupil region is extracted from the input image, now it is required to find the centre and radius of the pupil to define pupillary boundary. This can be computed by averaging coordinates of two end points of largest number of pixels of pupil region both in horizontal and vertical directions.

- a. Count the number of white pixels in each row and column of the detected pupil image.
- b. Determine row and column numbers, corresponding to maximum count of white pixels
- c. Find the coordinates of end pixels, corresponding to these row and columns.
- d. Intersection of lines made by joining these pixels in vertical and horizontal directions will depict the centre of pupil (x_c, y_c) .

Defining pupillary boundary:

Knowing the coordinates of the centre of the pupil, the radius of pupil region can be obtained as follows. Sum the pixel values of the binarized image in x and y directions to generate x-vector and y-vector

- a. Replace the nonzero values of x-vector and y-vector with 1s.
- b. Sum the x-vector and divide it by 2 to determine the radius (r_p)

Once the radius (r_p) of the pupil region is determined, a circle is defined around (x_c, y_c) with r_p as radius, to segment the pupil region and at the same time defining its boundary also.

2.2.3. Pupil segmentation in the presence of Glass Specular Reflection

Iris segmentation in the presence of Glass specular reflection is one of the trickiest problems for which the industry is searching for solutions. For iris segmentation or analysis, specular reflections which are produced because of light illumination adapted for capturing iris images at the time of image acquisition or from environ light reflections are big obstacles. When the images are captured from the persons wearing spectacles, the reflections from the glasses from various illuminating sources in nearby vicinity produces not only noisy bright spots on the image but also affects iris pattern gradation. If the reflection spots are concentrated around the pupil and iris regions, it becomes hazardous to segment the iris region and extract the features.

So here, Distance Adaptive Illumination Compensation Impainting Technique (DAICIT) was proposed to counter the problem mentioned above so that segmentation of pupil and iris can be carried effectively.

Algorithm:

- a. Binarize the image with suitable threshold to haul out the brightly illuminated regions.
- b. Supposing, X_k as the k^{th} block of the detected specular smudges in the binarized iris image, mine the largest luminous hunk X_1 from the remaining with suitable morphological operations.
- c. Determine the centroid (x_c, y_c) of the luminous hunk X_1 .
- d. With the help of spatial centre of pupil (x_p, y_p) , evaluate the distance, direction and effective spread of impact of this specular hunk on the iris region. The distance $vmag$ and direction $vang$ are estimated with magnitude and angle made by the vector framed between the centre of the pupil and centroid of the specular smudge.

$$vmag = \sqrt{(xc - xp)^2 + (yc - yp)^2} \quad (3)$$

$$vang = \tan^{-1} \left(\frac{yc - yp}{xc - xp} \right) \quad (4)$$

The effective angular spread of luminous intensity at iris region from specular hunk is determined by using the distance measure $vmag$ with the following equations

$$\theta_{_clock} = (vang - (360 - vmag) / 2) \quad (5)$$

$$\theta_{_anticlock} = (vang + (360 - vmag) / 2) \quad (6)$$

$$\text{Effective Spread: } \theta_{_es} = \theta_{_anticlock} - \theta_{_clock} \quad (7)$$

5. Now every pixel $I_i(i, j)$ in the effective spread of iris region is interpolated by mapping it with new value $I_{\text{new}}(i, j)$, computed by the equation

$$I_{\text{new}}(i, j) = I_i(i, j) - (k * I_i(i, j) / D) \quad (8)$$

$I_i(i, j)$ - pixel intensity at the i^{th} row and j^{th} column of iris region.

$I_{\text{new}}(i, j)$ - denote the impainting value of $I_i(i, j)$.

k- Scaling factor

D- The distance between the individual pixels to centroid of specular smudge.

The second parameter $(k * I_i(i, j) / D)$ reduces the original pixel intensity by some reasonable percentage to balance the intensity from the added brightness by specular hunk. This parameter is directly proportional to the intensity of the existing pixel and inversely proportional to the distance from the specular smudge. So, the percentage reduction in pixel intensity is well balanced as the spread of brightness varies with distance and the distance adapted here is independent for individual pixel.

2.3. Limbiac detection

After defining the pupillary boundary, it is requisite now to estimate outer limbiac boundary, for the extraction of the iris region. Unlike pupillary boundary, the detection of limbiac boundary, which separates iris from sclera, is very difficult and sensitive issue, as the transition of gray intensities from iris to sclera is very smooth. So the iris region is alienated into circular clusters around the pupil centre and the pixels of cluster are substituted with the mean of cluster pixels, to make the gray intensities distinguishable between iris and sclera. Most of the time the top and bottom areas of the iris are occluded by eyelashes and eyelids, so the limbiac boundary is estimated from the area covered between the top and the bottom edge points of pupil region along the horizontal direction. An edge detection algorithm using principle of maximum gradient difference between post mean substituted gray levels of succeeding circumferences is used to estimate the outer boundary of iris, i.e. limbiac boundary of iris. Here it is assumed that pupil and iris are circular in shape and share the same centre an integro differential operator is used for this purpose.

$$\max_{(r, x_c, y_c)} \left| P(r) * \left[\oint_{(r, x_c, y_c)} \frac{I(x, y)}{2\pi r} ds \right] \right| \quad (9)$$

The operator behaves as circular edge detector that searches for maximum contour integral derivative with increasing radius on concentric circles successively. In execution, the contour fitting procedure is discretized, with finite sums serving for integration and finite differences between successive circles serving for derivatives. Maximum of difference of post mean substituted value is used to create maximum gray scale value at the iris-sclera boundary. Fitting contours to images using such optimization formulation, which is a standard machine vision technique is often referred to as active contour modeling. First, the mean of gray values of pixels on virtual circles are computed, by incrementing the radius in steps, from the centre of the pupil and a vector is formed with these mean values, $m = \{ m_1, m_2, \dots, m_n \}$. A new vector $v_pms = \{ v_1, v_2, \dots, v_n \}$ is generated with the present value being replaced with the post mean values of intensities of virtual circles, using the formula

$$V_p = \frac{1}{n} \sum_{k=p}^{p+n} m_k \quad (10)$$

Or

$$v_p = (m_{p+1} + m_{p+2} + m_{p+3} + \dots + m_{p+n})/n$$

Generate weighed mean vector $v_wpms = \{ wv_1, wv_2, \dots, wv_n \}$ that holds post mean substituted pixel intensities of the virtual circles multiplied by the weights. The weights that were accommodated were nothing but the positions of the virtual circles from the centre of pupil. The difference vector $vd_wpms = \{ vd_1, vd_2, \dots, vd_n \}$ is adapted to create the difference between the successive circles in order to project the biggest difference at iris-sclera boundary. Position of maximum value in vd_wpms vector, determines the radius of limbiac region. The maximum value endows the maximum blur representing the separation of iris region from sclera, and position of this maximum value represents the radius of limbiac boundary.

Since the sclera gray intensities will be higher than that of iris pixel intensities, the virtual circle at iris-sclera boundary will be bestowed with maximum value, i.e., difference of weighted post mean substitution brings maximum value of blur at transitions of boundaries between sclera and iris. This maximum value of blur above the pupillary region gives the limbiac position and the distance from the centre of the pupil to limbiac position gives the radius of outer iris region. The sweep of sequence to detect limbiac boundary are itemized with the following steps.

- a. Locate the centre (x_p, y_p) and radius (r_p) of the pupil using IITCE algorithm.
- b. Isolate horizontal strip covering pupil region.
- c. Create vector $m = \{ m_1, m_2, \dots, m_n \}$ that holds mean pixel intensities of the virtual circles fleeting around the centre of the pupil by using integro differential operator.
- d. Create vector $v_pms = \{ v_1, v_2, \dots, v_n \}$ that holds post mean substituted pixel intensities of the virtual circles by applying PMS.
- e. Generate vector $v_wpms = \{ wv_1, wv_2, \dots, wv_n \}$ which holds weighed PMS values.
- f. Generate difference vector $vd_wpms = \{ vd_1, vd_2, \dots, vd_n \}$ which gives the difference between the successive values of v_wpms .
- g. Determine the maximum value and its position in vd_wpms vector.

- h. Position of maximum value gives the radius of limbiac boundary.

Once the inner and outer peripheries of iris are determined in the name of pupillary and limbiac boundaries, iris is extracted, by marking all the remaining pixels in the image, to gray value 255 (white) or to gray value 0 (black).

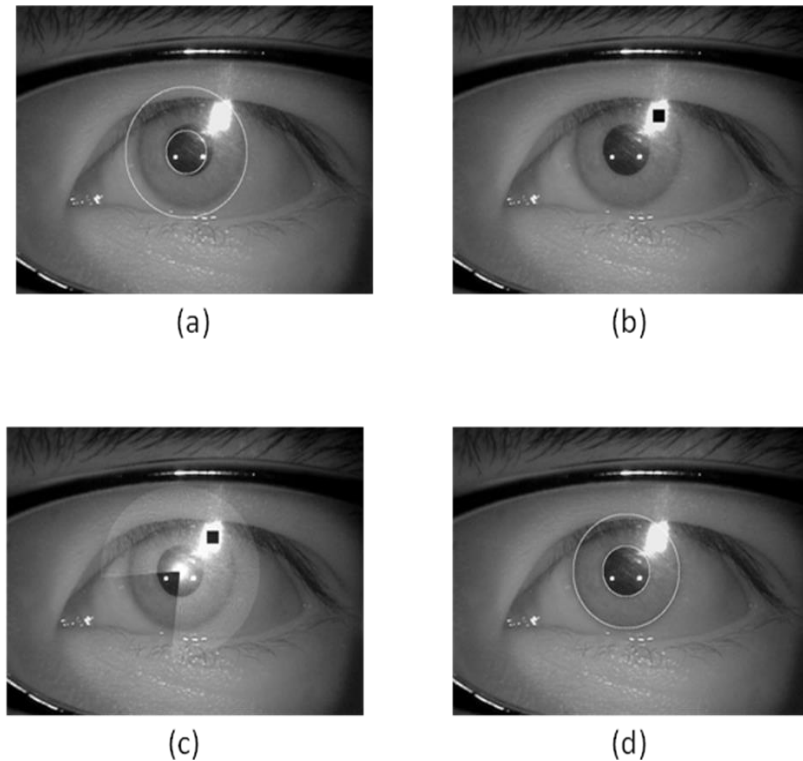


Figure 3. (a) Iris localization without DAICIT; (b) locating centroid;
(c) Defining DAICIT spread; (d) Iris localization with DAICIT.

Once iris is segregated and extracted from the eye image, it is carried to normalization process where, each point in the iris region is mapped to a pair of polar coordinates, forming a fixed size unwrapped rectangular iris image

3. Experimental Results

3.1. Datasets

In order to promote research on long-range and large-scale iris recognition systems, CASIA released CASIA Iris Image Database V4.0 (CASIA-IrisV4), to the public domain. CASIA-IrisV4 contains a total of 54,601 iris images from more than 1,800 genuine subjects and 1,000 virtual subjects. All iris images are 8 bit gray-level JPEG files, collected under near infrared illumination or synthesized. CASIA_IrisV4 is an extension of CASIA-IrisV3 and contains six subsets named as CASIA-IrisV3 are CASIA-Iris-Interval, CASIA-Iris-Lamp, and CASIA-Iris-Twins, CASIA-Iris-Distance, CASIA-Iris-Thousand, and CASIA-Iris-Syn. CASIA-Iris-Interval, CASIA-Iris-Lamp, and CASIA_Iris_Thousand databases are chosen to evaluate the performance of proposed algorithms.

3.1.1. CASIA Iris Interval

High clarity iris images with resolution 320x280, were captured with close-up iris camera in indoor environment in two sessions.

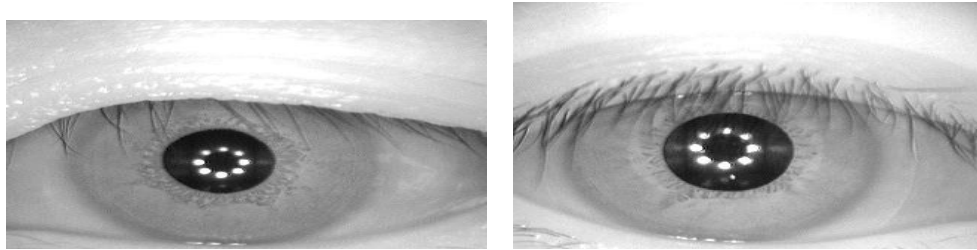


Figure 4. CASIA-Iris-Interval

The images are most suitable to study the texture features of iris. The database contains 2639 images of 249 subjects, breeding 395 classes.

3.1.2. CASIA Iris Lamp

One of the most challenging issues in iris recognition is deformation of iris texture with dilation of pupil. Variation of illumination forces the pupil to expand or contract, in turn alters the pattern of iris and makes the recognition of individual, an issue. CASIA-Iris-Lamp produced intra class variation of iris images with dilation of pupil, which is best suited to study the problems of non linear deformation of texture due to variations in illumination.

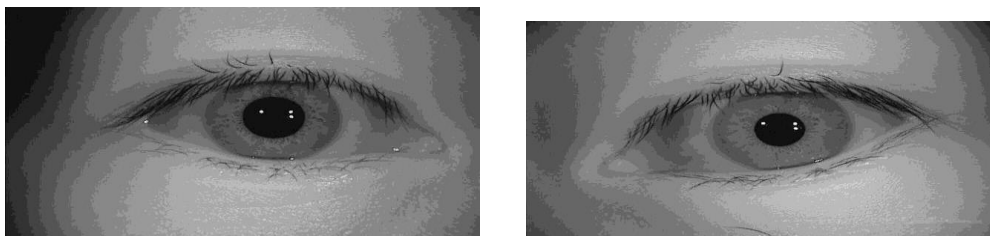


Figure 5. CASIA-Iris-Lamp

Dilation of pupil was customized by turning a lamp on/off, close to the eye using a hand-held iris sensor produced by OKI. CASIA-Iris-Lamp database was fortified with 16,212 iris images of 640x480 resolution, of 411 subjects.

3.1.3 CASIA Iris Thousand

CASIA-Iris-Thousand is the first publicly available dataset with more than 1000 subjects containing 20000 images. To the best the database is fortified with 2000 classes, which is best suited for developing iris classification and indexing methods. The fundamental sources posing intra class variations in the database are specular reflections and eye glasses.

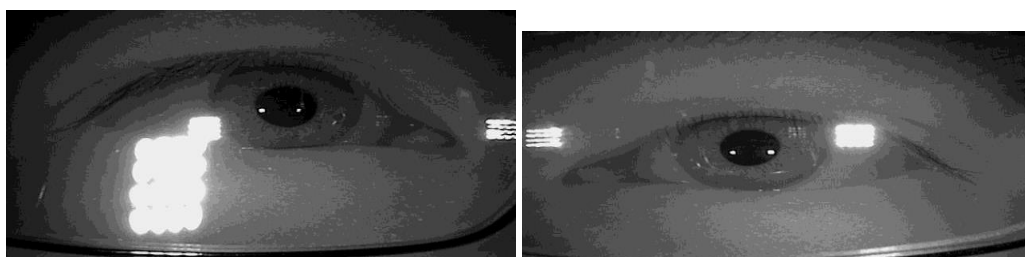


Figure 6. CASIA-Iris-Thousand

The iris images of wide range distribution of ages, with 640x480 resolution, were captured indoor with lamp on/off using Iris King IKEMB-100 camera, which is user friendly dual eye camera provided with bounding boxes in frontal LCD, to adjust the position of eye, in the acquisition of high quality iris images.

3.2. Performance Evaluation

The performance of the proposed algorithms for segmentation, feature extraction and recognition in identification of iris are evaluated in this section. CASIA_Iris_Interval, CASIA_Iris_Lamp, CASIA_Iris_Thousand database are used for this purpose.

3.2.1. Evaluation of proposed segmentation model

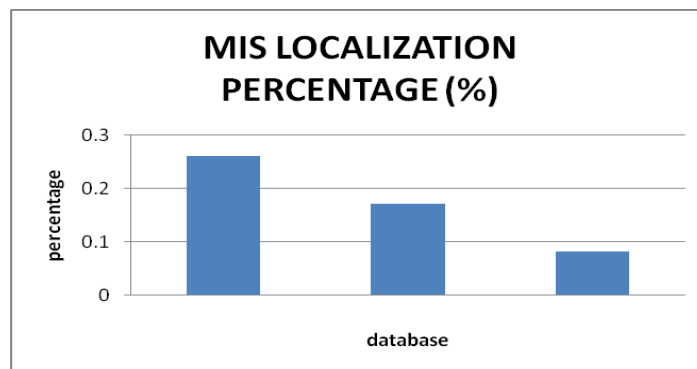
The mislocalization percentage in segmentation and average localization time required to segment iris from the eye images are evaluated on CASIA-Iris V4 database.

Table 1. Comparison of mislocalization percentage (i) on CASIA_IrisV4 database (ii) with other existing methods

Mislocalization Percentage – CASIA-Iris V4 - Comparison	
DATABASE	Mislocalization Percentage (%)
CASIA_Iris_Interval	0.26 %
CASIA_Iris_Lamp	0.17 %
CASIA_Iris_Thousand	0.075 %

(i)

Mislocalization Percentage – Comparison with Existing Methods.			
DATABASE	MASEK	MEHROTRA	PROPOSED
CASIA_Iris_Interval	5.23 %	0.45 %	0.26 %



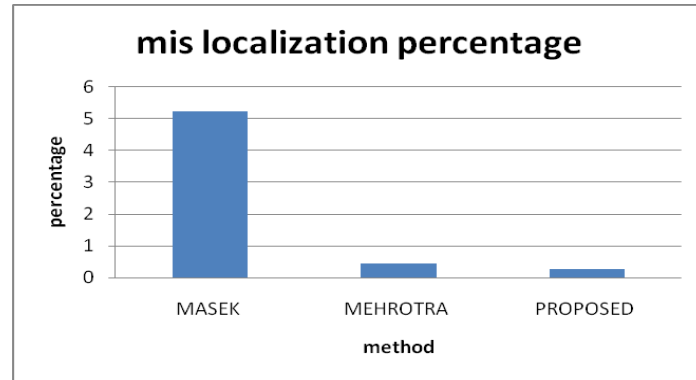


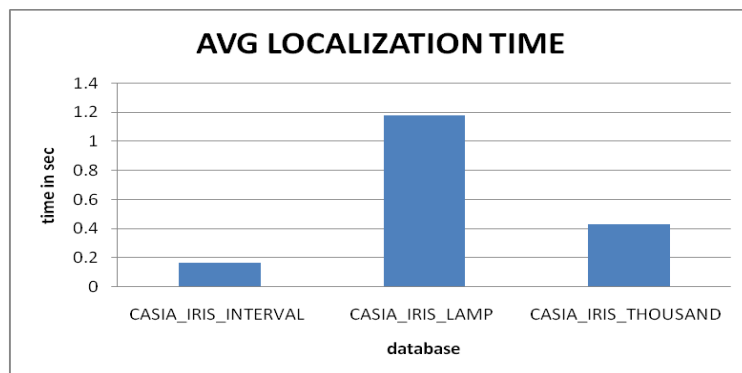
Figure 7. Graphical Representation for comparison of the mislocalization percentage (i) CASIA-IrisV4 database (ii) with existing methods

Table 2. Comparison of average localization time (i) on CASIA-IrisV4 database (ii) with existing methods

Database	Average Localization Time
CASIA-Iris-Interval	0.16 sec
CASIA-Iris-Lamp	1.18 sec
CASIA-Iris-Thousand	0.43 sec

(i)

Average Localization Time- Comparison with Existing Methods.			
DATABASE	MASEK	MEHROTRA	PROPOSED
CASIA_Iris_Interval	13.067 sec	0.396 sec	0.16 sec



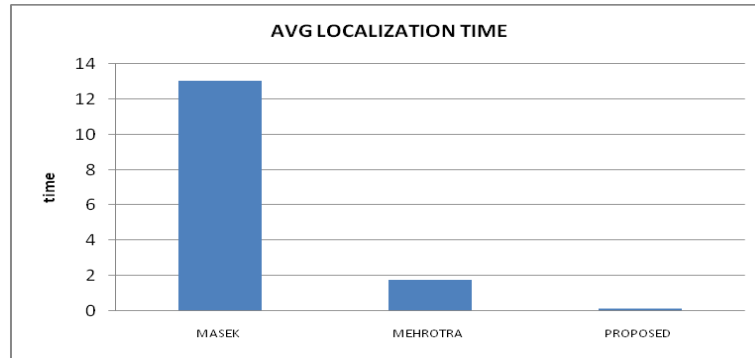


Figure 8. Graphical Representation for comparison of the average localization time (i) CASIA-IrisV4 database (ii) with existing methods

The results tabulated in table 1 (i) and their graphical representations in figure 7 (i) compares the mislocalization percentage in segmentation of irises on casia v4 database. The misclassification percentage in segmentation obtained by the proposed technique on Casia-Iris-Interval, Casia-Iris-Lamp and Casia-Iris-Thousand database is 0.26, 0.17 and 0.075 respectively. The results tabulated in table 2 (i) and their graphical representations in figure 8 (i) compares the average localization time of segmentation of irises on CASIA-IrisV4 database. The proposed technique segments CASIA-Iris-Interval, CASIA-Iris-Lamp and CASIA-Iris-Thousand database with time spans of 0.16 sec, 1.18 sec and 0.43 sec respectively.

The results tabulated in table 1(ii) and their graphical representations in figure 7 (ii) compares the performance of segmentation of irises with Masek’s bench mark algorithm and Mehrotra’s [3] approach. Masek’s approach utilizes Circular Hough Transform, to localize both pupil and limbic boundaries. It works well on localizing pupil boundary to that of limbiac boundary in most of the cases of CASIA-Iris-Interval database. Its performance in localizing iris, fails drastically on low resolution and noisy images. Table 1(ii) elucidates the improvement in mislocalization percentage of 0.26 of proposed approach over 5.23 of Masek’s approach and 0.45 of Mehrotra’s.

Table 2(ii) shows the average time taken by Masek’s approach to segment iris from the image is approximately 13.06 seconds per image. The approach adapted by Mehrotra et al [12], utilizes a non parametric spectrum approach to localize the pupil and circular summation of intensity approach to localize limbiac boundary. The algorithm proposed by Mehrotra segments iris with in 0.396 sec which is much faster to Masek’s approach. The proposed algorithm was able to segment the iris with average time of 0.16 sec which excels both the above said approaches.

As said above in introduction, Hough transform needs very large data and number of iterations in finding the circular portions of pupil as well as of iris for large range of radius values. The computations required become very expensive for high resolution images, resulting in reduced speed which is the main drawback of Masek’s approach. In case of Mehrotra’s approach, though the pupil segmentation approach was novel and innovative, it consumes moderate time for the required processing. Whereas the proposed iterative approach was able to overcome most of the difficulties with the support of preprocessing and weighted post mean substitution approach in the detection of iris region, and performed remarkably both in reducing mislocalization percentage as well as reducing the detection time with reasonable accuracy.

Table 3. Segmentation performance of proposed technique on noisy images

Database	Noisy Images	Segmented Correctly	Percentage	Avg Time
CASIA_Iris_Thousand	1000	996	99.6	4.43 sec

The tabulated results in table 3 show the proposed technique's performance on noisy images existing in Casia-Iris-Thousand database. Cassia-Iris-Thousand database contains most noisy images with specular reflection of glasses, challenging the segmentation process. The proposed algorithm is applied on selected thousand images and results are tabulated in table 3. It is found that the proposed algorithm segments the noisy database correctly to the extent of 99.6% and the average time taken per iris to be localized is 4.43 sec.

References

- [1] J. G. Daugman. "High confidence visual recognition of persons by a test of statistical independence". IEEE Transaction on Pattern Analysis and Machine Intelligence, vol.5,no.11,(1993),pp.1148–1161.
- [2] Richard P. Wildes, "Iris Recognition: An Emerging biometric Technology", In Proceedings of the IEEE, vol. 85, no.9, (1997),pp.1348-1363
- [3] John Daugman, "How Iris Recognition Works", IEEE Transactions on Circuits And Systems For Video Technology, vol. 14, no.1,(2004) ,pp. 21-30.
- [4] Xiaoyan Yuan, Pengfei Shi, "Iris Feature Extraction Using 2D Phase Congruency", Proceedings of the Third International Conference on Information Technology and Applications (ICITA'05,(2005).
- [5] Peng Yao, Jun Li, Xueyi Ye, Zhenquan Zhuang, Bin Li, "Iris Recognition Algorithm Using Modified Log-Gabor Filters", (2006).
- [6] John Daugman, "New Methods in Iris Recognition", IEEE Transactions on Systems, Man and Cybernetics Part B: Cybernetics, vol. 37, no. 5,(2007), pp. 1167-1175.
- [7] Mayank Vatsa, Richa Singh, Afzel Noore," Improving Iris Recognition Performance Using Segmentation, Quality Enhancement, Match Score Fusion, and Indexing", IEEE transactions on systems, man, and cybernetics—part b: cybernetics, vol. 38, no. 4, (2008).
- [8] N. Popescu-Bodorin, "Exploring New Directions in Iris Recognition", in Proc. 11th Conf. Symbolic and Numeric Algorithms for Scientific Computing, September (2009).
- [9] Bava Elizabeth Mathew, "Securing Web Services by Iris Recognition System", International Journal of Computer Applications, vol. 13, no.7, (2011),pp. 23-28.
- [10] R. P. Wildes, J. C. Asmuth, G. L. Green, and S. C. Hsu. "A system for automated iris recognition", In Proceedings of the Second IEEE Workshop on Application of Computer Vision, (1994), pp. 121–128.
- [11] Mehrotra, Sa and Majhi, "Fast segmentation and adaptive SURF descriptor for iris recognition", Mathematical and Computer Modelling, vol. 58, no.1,(2013) ,pp.132-146.
- [12] Wei-Yu Han, Wei-Kuei Che1, Yen-Po Lee, Kuang-shyr Wu and Jen-Chun Lee, "Iris Recognition based on Local Mean Decomposition", Appl. Math. Inf. Sci,vol.8, no. 11, (2014), pp.217-222.
- [13] Ali Azimi Kashani , Alimohamad Monjezi Nori, Iman Mosavian, "New methods of verification and identification using iris patterns", Journal of Scientific Research and Development,vol. 2,no.3,(2015),pp.118-122.
- [14] Boles and Boalshash, "A Human Identification Technique Using images of the Iris and Wavelet Transform", IEEE Transactions on Signal Processing, vol.46, no 4, (1998),pp. 185-1188.
- [15] Samir Shah and Arun Ross," Iris Segmentation Using Geodesic Active Contours", IEEE TRANSACTIONS ON INFORMATION FORENSICS AND SECURITY, vol. 4, no. 4, (2009).
- [16] Samata Kharul, Uttam Chaskar, " Quality Factors Estimation Of Iris Images", Int. J. of Recent Trends in Engineering & Technology, vol. 11, (2014).
- [17] M. Hogan, J. Alvarado, and J.Weddell, "Histology of the human eye", W.B. Saunders,(1971).

- [18] Richard P. Wildes, “Iris recognition: an emerging biometric technology”, In: Proc. of the IEEE, vol.85,no.9, (1997),pp.1348-1363.
- [19] J. Daugman, High confidence visual recognition of persons by a test of statistical independence, IEEE Transactions on Pattern Analysis and Machine Intelligence,vol. 15,no.11, (1993),pp. 1148–1161.
- [20] R. Wildes, J. Asmuth, G. Green, S. Hsu, R. Kolczynski, J. Matey, “A system for automated iris recognition”, In: Proc. IEEE Workshop on Applications of Computer Vision ,Sarasota, FL, (1994),pp.121-128.
- [21] R. Wildes, Iris recognition: an emerging biometric technology, Proceedings IEEE,vol. 85,no.9, (1997),pp. 1348–1363.
- [22] W. Boles, B. Boashash, A human identification technique using images of the iris and wavelet transform, IEEE Transactions on Signal Processing ,vol.46,no.4, (1998),pp. 1185–1188.
- [23] W. K Kong and D. Zhang, “Accurate iris segmentation method based on novel reflection and eyelash detection model”, In: Proc. International Symposium on Intelligent Multimedia, Video and Speech Processing, HongKong,(2001), pp.263 - 266.
- [24] Li Ma, Tieniu Tan, Yunhong Wang, and Dexin Zhang, “Personal identification based on iris texture analysis”, IEEE Transactions on Pattern Analysis and Machine Intelligence, vol..25, no.12, (2003), pp.1519-1533.
- [25] Libor Masek, “Recognition of human iris patterns for biometric identification”, The University of Western Australia, (2003).
- [26] L. Masek, P. Kovesei, Matlab source code for a biometric identification system based on iris patterns, The School of Computer Science and Software Engineering, The University of Western Australia, (2003).
- [27] John G. Daugman, “How iris recognition works”, IEEE Transactions on Circuits and Systems for Video Technology, vol.14, no.1, (2004), pp.21-30.
- [28] S. P. Narote, A. S. Narote, L. M. Waghmare, “Iris recognition technology”, In: Proc. International Conference on Cognition, and Recognition, Mysore, India, (2005), pp. 863 - 868.
- [29] S. P. Narote , A. S. Narote , L. M. Waghmare “An Automated Iris Image Localization in Eye Images used for Personal Identification”, 14 th international conference on advanced computing and communication,(2006),June 6-8.
- [30] R. Gonzalez, R. Woods, Digital Image Processing, third ed., Prentice Hall, (2007).
- [31] Casia database. <http://www.cbsr.ia.ac.cn/english/Databases.asp>.